

FRAME DEPENDENCE OF THE ELECTRIC FIELD SPECTRUM OF SOLAR WIND TURBULENCE

C. H. K. CHEN¹, S. D. BALE^{1,2}, C. SALEM¹, AND F. S. MOZER¹¹Space Sciences Laboratory, University of California, Berkeley, CA 94720, USA; chen@ssl.berkeley.edu²Physics Department, University of California, Berkeley, CA 94720, USA

ABSTRACT

We present the first survey of electric field data using the *ARTEMIS* spacecraft in the solar wind to study inertial range turbulence. It was found that the average perpendicular spectral index of the electric field depends on the frame of measurement. In the spacecraft frame it is $-5/3$, which matches the magnetic field due to the large solar wind speed in Lorentz transformation. In the mean solar wind frame, the electric field is primarily due to the perpendicular velocity fluctuations and has a spectral index slightly shallower than $-3/2$, which is close to the scaling of the velocity. These results are an independent confirmation of the difference in scaling between the velocity and magnetic field, which is not currently well understood. The spectral index of the compressive fluctuations was also measured and found to be close to $-5/3$, suggesting that they are not only passive to the velocity but may also interact nonlinearly with the magnetic field.

Subject headings: magnetic fields – magnetohydrodynamics (MHD) – plasmas – solar wind – turbulence

1. INTRODUCTION

The solar wind is a plasma that is observed to be turbulent with fluctuations at a broad range of scales (Tu & Marsch 1995; Goldstein et al. 1995; Horbury et al. 2005; Bruno & Carbone 2005; Petrosyan et al. 2010). It is usually modeled as a cascade of energy from large scales (e.g., Wicks et al. 2010), where the energy is injected, to small scales (e.g., Chen et al. 2010a), where kinetic processes dissipate the energy (e.g., Schekochihin et al. 2009). The inertial range fluctuations are thought to be primarily Alfvénic in nature, with Alfvén-wave-like polarizations (Belcher & Davis 1971) and phase speeds close to the Alfvén speed (Bale et al. 2005).

There are various theories of Alfvénic turbulence, based on interacting packets of Alfvén waves. The theory of Goldreich & Sridhar (1995), based on critical balance, predicts that the Alfvénic fluctuations have a perpendicular one-dimensional energy spectrum $E(k_{\perp}) \sim k_{\perp}^{-5/3}$, where k_{\perp} is the wavevector perpendicular to the magnetic field. The theory of Boldyrev (2006), which in addition assumes scale-dependent alignment, predicts that their spectrum is $E(k_{\perp}) \sim k_{\perp}^{-3/2}$. Similar predictions also exist for the multitude of imbalanced theories (e.g., Lithwick et al. 2007; Beresnyak & Lazarian 2008; Chandran 2008; Perez & Boldyrev 2009; Podesta & Bhattacharjee 2010; Podesta 2011).

In the solar wind at 1 AU, it has been shown that the spectral index of the magnetic field is close to $-5/3$ on average but that the spectral index of the velocity is closer to $-3/2$ (e.g., Mangeney et al. 2001; Podesta et al. 2007; Salem et al. 2009; Tessein et al. 2009; Podesta & Borovsky 2010; Wicks et al. 2011). This difference between the two fields is not consistent with any of the current theories of Alfvénic turbulence and is one of the currently unsolved problems of solar wind turbulence.

Past measurements of the electric field spectrum in the frame of the spacecraft found it to closely match the magnetic field (Bale et al. 2005; Sahraoui et al. 2009). These measurements used single intervals of data but it has been shown (e.g., Tessein et al. 2009) that the velocity and magnetic field have a large spread of spectral indices and many intervals are needed

to determine the average behavior.

In this Letter, we present a survey of electric field measurements in the solar wind using many intervals of data. We explain why the electric field in the spacecraft frame follows the magnetic field and make new measurements of the electric field in the mean solar wind frame. In Section 2, we describe the data set, in Section 3 we discuss our results and in Section 4 we present our conclusions.

2. DATA SET

We used data from the *ARTEMIS* mission (Angelopoulos 2010), which is an extension of the *THEMIS* mission (Angelopoulos 2008). During late 2010, the two *ARTEMIS* spacecraft (*P1* and *P2*) moved from equatorial Earth orbits to Lunar Lagrange orbits ($\sim 60 R_E$ from the Earth). Periods of solar wind data were selected in which each spacecraft was upstream of the Moon, out of Earth’s ion foreshock and the required instruments were operational. The selected days are: days 245–257, 308–310, 316–318, 337–343 of 2010 and days 1–3, 40–42 of 2011 for *P1*; days 217–230, 275–284, 304–307, 361–364 of 2010 and days 25–28 of 2011 for *P2*. The same day in both spacecraft was avoided so that the intervals are independent. All of the data from these days were split into 6 hr sections resulting in 272 intervals, 98% of which were in slow solar wind ($< 500 \text{ km s}^{-1}$).

Spin resolution ($\sim 3 \text{ s}$) electric field data, \mathbf{E}_{sc} , from the electric field instrument (EFI; Bonnell et al. 2008) was used, along with spin resolution magnetic field data, \mathbf{B} , from the fluxgate magnetometer (FGM; Auster et al. 2008) and varying resolution ion velocity, \mathbf{v} , and ion number density, n , onboard moments from the electrostatic analyzer (ESA; McFadden et al. 2008). A despun spacecraft coordinate system (DSL) was used, in which z is the spacecraft spin axis. The DSL system for *ARTEMIS* is approximately the same as the geocentric solar ecliptic (GSE) system with the sign of the y - and z - axes reversed. The wire boom electric field antennas are in the x - y plane and extend a few Debye lengths from the spacecraft. Data with the currently most recent calibrations (v01) were used for all instruments.

For \mathbf{E}_{sc} it was found that some extra calibration was needed. A least-squares fit, varying the $E_{y,\text{sc}}$ offset O_{E_y} and the \mathbf{E}_{sc} scaling factor F , was performed to minimize the difference

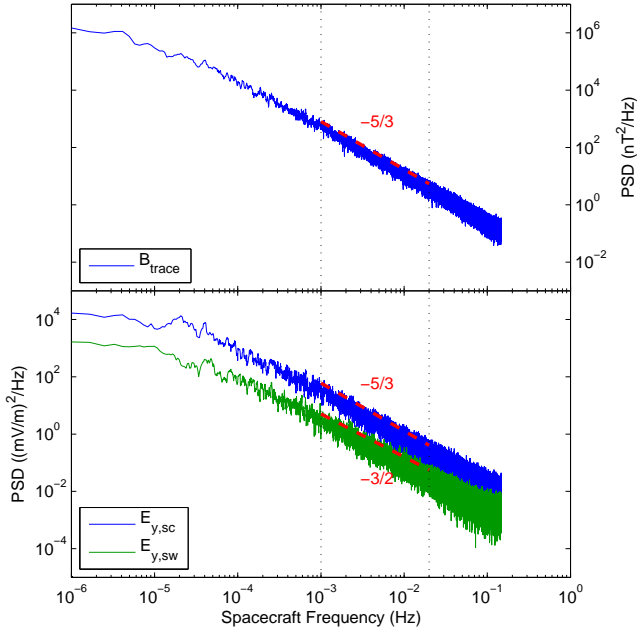


Figure 1. Sample power spectra from *P2* 2010 days 217–230. The dotted lines show the range of scales that the spectral index is fitted to. Gradients of $-5/3$ and $-3/2$ are marked for reference.

between $E_{y,sc}$ and the y -component of $-\mathbf{v} \times \mathbf{B}$ for each interval (this technique assumes ideal MHD). Each 6 hr interval was corrected using these empirically determined values. The mean value of O_{E_y} was found to be -0.17 mV m^{-1} for *P1* and -0.23 mV m^{-1} for *P2*; the mean value of F was found to be 1.02 for *P1* and 0.99 for *P2*. An alternative fit using a B_z offset instead of an $E_{y,sc}$ offset was also tried, resulting in B_z offsets $\sim 0.6 \text{ nT}$. The results of this Letter, however, are not significantly affected by either of these additional calibration methods.

The velocity and density data was cleaned up by removing unphysical spikes and other spurious data that was present. This was done by linearly interpolating over data points more than 4 standard deviations from the mean in each 6 hr interval (this process was repeated three times for each interval). Any data gaps in the 3 s resolution data were also linearly interpolated over to produce time series with consistent 3 s resolution. After this process, occasional small spikes, sometimes seen in all three instruments, remained in the time series of some intervals. These are likely due to noise but did not affect this analysis (excluding these intervals did not significantly change the results of this Letter).

The electric field was measured in the frame of the spacecraft, \mathbf{E}_{sc} , and converted into the frame of the mean solar wind velocity, \mathbf{E}_{sw} , using the Lorentz transformation,

$$\mathbf{E}_{sw} = \mathbf{E}_{sc} + \mathbf{v}_{sw} \times \mathbf{B}, \quad (1)$$

where \mathbf{v}_{sw} is the mean solar wind velocity relative to the spacecraft over each interval ($\mathbf{v} = \mathbf{v}_{sw} + \delta\mathbf{v}$). Since \mathbf{B} is a fluctuating quantity, it was linearly interpolated onto the times of \mathbf{E}_{sc} so that the transformation could be done for each electric field measurement.

The power spectrum of each component of \mathbf{B} and \mathbf{v} , of the x - and y - components of \mathbf{E}_{sc} and \mathbf{E}_{sw} , of the magnetic field

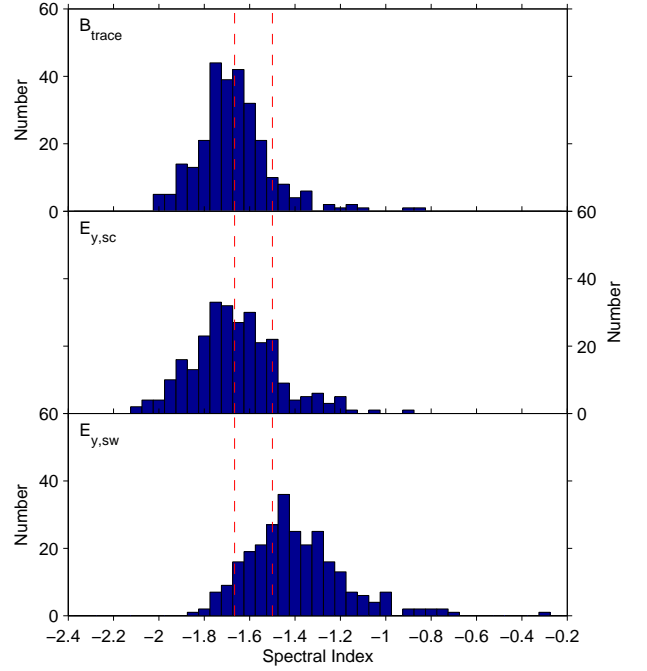


Figure 2. Histograms of spectral index for the trace of the magnetic field and the y -component of the electric field in the spacecraft and mean solar wind frames. Values of $-5/3$ and $-3/2$ are marked for reference.

magnitude $|\mathbf{B}|$, and of n was calculated for each of the intervals. The multitaper method with time-bandwidth product $NW = 4$ and 7 eigentapers (Percival & Walden 1993) was used (using a standard Fourier transform does not affect the results to within errors). Typical power spectra for a longer interval (14 days) are shown in Figure 1: the trace of the magnetic field spectrum and the y -component of the electric field spectrum in both frames. Since the solar wind fluctuations are anisotropic with $k_{\perp} > k_{\parallel}$ (e.g., Chen et al. 2010b), these are measurements of the perpendicular spectrum $E(k_{\perp})$ (to measure $E(k_{\parallel})$ a local field tracking technique would be needed (e.g., Horbury et al. 2008; Chen et al. 2011)).

Each spectral index was determined from the gradient of the best-fit line to the power spectrum in log-log space over the spacecraft frequency range $1 \times 10^{-3} \text{ Hz}$ to $2 \times 10^{-2} \text{ Hz}$ (marked as dotted lines in Figure 1). Applying Taylor’s hypothesis (Taylor 1938) since the solar wind is super-Alfvénic, this range corresponds approximately to scales 18,000 km to 350,000 km and a perpendicular wavevector range $0.0018 < k_{\perp} \rho_i < 0.036$, where $\rho_i \approx 100 \text{ km}$ is the typical ion gyroradius. This is in the middle of the inertial range and was chosen because good power laws exist here in all intervals. The results of the analysis are described in the next section.

3. RESULTS

Histograms of the spectral indices for the magnetic and electric fields are shown in Figure 2. The magnetic field trace spectral index histogram can be seen to peak close to $-5/3$, in agreement with previous results (e.g., Smith et al. 2006; Tessein et al. 2009). The histogram of the y -component of the electric field in the spacecraft frame also peaks near $-5/3$ but the histogram of the same component in the mean solar wind frame peaks closer to $-3/2$.

Table 1
Mean Spectral Indices

Field	Spectral Index
B_{trace}	-1.67 ± 0.01
v_{trace}	-1.50 ± 0.02
$E_{y,\text{sc}}$	-1.66 ± 0.01
$E_{x,\text{sc}}$	-1.45 ± 0.01
$E_{y,\text{sw}}$	-1.40 ± 0.01
$E_{x,\text{sw}}$	-1.39 ± 0.01
$ \mathbf{B} $	-1.64 ± 0.01
n	-1.63 ± 0.02

The mean spectral indices for each field are given in Table 1, along with the standard error of the mean σ/\sqrt{N} , where σ is the sample standard deviation and N is the number of intervals. The mean velocity and density spectral indices were calculated from only 117 and 120 of the intervals, respectively. These are the intervals for which 3 s onboard moment data was available and no more than 5% of the data was missing. This explains the larger error for these fields. The same analysis was also tried with 24 hr intervals (not shown here), resulting in a smaller spread of spectral indices but the same mean values to within 2 standard errors.

The fact that the scaling of $E_{y,\text{sc}}$ matches B_{trace} can be shown to be due to the Lorentz transformation. In ideal MHD, the three fields are related to each other in the mean solar wind frame by $\mathbf{E}_{\text{sw}} = -\delta\mathbf{v} \times \mathbf{B}$ and putting this into Equation (1) gives

$$\mathbf{E}_{\text{sc}} = -\delta\mathbf{v} \times \mathbf{B} - \mathbf{v}_{\text{sw}} \times \mathbf{B}. \quad (2)$$

Since the mean solar wind speed is much larger than the fluctuations, $|\mathbf{v}_{\text{sw}}| > |\delta\mathbf{v}|$, and is mostly in the x (radial) direction, $E_{y,\text{sc}}$ is dominated by the magnetic field fluctuations convected by the mean solar wind flow and therefore follows their scaling. The amplitudes of the spectra in Figure 1 agree with this interpretation: the $E_{y,\text{sc}}$ spectrum is an order of magnitude larger than the $E_{y,\text{sw}}$ spectrum, showing that for the y -component, the second term on the right-hand side of Equation (2) is larger than the first. The x -component of Eq. 2 does not depend on the radial solar wind velocity, so scaling of $E_{x,\text{sc}}$ does not depend only on the scaling of \mathbf{B} and indeed is different to that of B_{trace} .

\mathbf{E}_{sw} has a scaling closer to that of v_{trace} , which can also be shown to be consistent with Alfvénic fluctuations in ideal MHD. Splitting the magnetic field into a constant mean value plus fluctuations, $\mathbf{B} = \mathbf{B}_0 + \delta\mathbf{B}$, the electric field in the mean solar wind frame is given by

$$\mathbf{E}_{\text{sw}} = -\delta\mathbf{v} \times (\mathbf{B}_0 + \delta\mathbf{B}). \quad (3)$$

The mean value of $|\delta\mathbf{B}|/|\mathbf{B}_0|$ is between 0.1 and 0.4 for the range of scales to which spectral indices were fitted. Since at these small scales in the solar wind $\mathbf{B}_0 > \delta\mathbf{B}$, the electric field spectrum in the mean solar wind frame is dominated by the velocity fluctuations, and therefore has a similar scaling. Similar arguments can be made for the Alfvénic fluctuations in gyrokinetic theory (Schekochihin et al. 2009). The fact that we observe a spectral index close to $-3/2$ in $E_{x,\text{sw}}$ and $E_{y,\text{sw}}$ also suggests that the perpendicular velocity component has this scaling, which is in agreement with the results of Chapman & Hnat (2007). The electric field scaling is also in agreement with previous measurements of the velocity trace spectral index (e.g., Tessein et al. 2009; Podesta & Borovsky 2010).

Table 2
Correlations Between Spectral Indices

Field 1	Field 2	Correlation Coefficient
B_{trace}	$E_{y,\text{sc}}$	0.82
B_{trace}	$E_{y,\text{sw}}$	0.15
B_{trace}	$E_{x,\text{sc}}$	0.24
B_{trace}	$E_{x,\text{sw}}$	0.08
$E_{y,\text{sc}}$	$E_{y,\text{sw}}$	0.17
$E_{y,\text{sc}}$	$E_{x,\text{sc}}$	0.24
$E_{y,\text{sc}}$	$E_{x,\text{sw}}$	0.14
$E_{y,\text{sw}}$	$E_{x,\text{sc}}$	0.38
$E_{y,\text{sw}}$	$E_{x,\text{sw}}$	0.36
$E_{x,\text{sc}}$	$E_{x,\text{sw}}$	0.86

The scaling of the compressive fluctuations ($|\mathbf{B}|$ and n) is close to $-5/3$, matching the trace magnetic field spectrum, rather than the velocity spectrum. Previous observations (e.g., Marsch & Tu 1990; Bellamy et al. 2005; Issautier et al. 2010) could not distinguish between $-5/3$ and $-3/2$ in the compressive fluctuations so this scaling is consistent with those observations. The compressive fluctuations are mainly due to the slow mode (Howes et al. 2011) and are sometimes thought to be passive to the Alfvénic turbulence. Since their scaling matches the magnetic field, rather than the velocity, the nonlinearity cannot be due solely to passive convection and may include nonlinearities with the magnetic field. This supports the theories of compressible reduced MHD and kinetic reduced MHD (Schekochihin et al. 2009), in which the compressive fluctuations interact nonlinearly with both the magnetic field and velocity.

To test the significance of the difference between the mean spectral index values in Table 1, the t -test was applied. This is appropriate since the spectral indices appear to be normally distributed and are independent measurements. The t value for differentiating between the spectral indices of B_{trace} and $E_{y,\text{sc}}$ is $t = 0.41$. This is smaller than the 95% value of 1.96 for infinite degrees of freedom, showing that there is no statistically significant difference between the scaling of these two fields. For differentiating between the spectral indices of $E_{y,\text{sw}}$ and $E_{y,\text{sc}}$ the t value is $t = 15$, larger than the 95% value, showing that these two fields have significantly different spectral indices. This confirms that the $-5/3$ and $-3/2$ difference is a statistically robust result.

To examine the cause of the spread of spectral index values, the correlation between the different spectral indices was measured. The linear correlation coefficients, calculated from various pairs of sets of the 272 spectral index values of each field, are shown in Table 2. It can be seen that the spectral indices of most pairs of fields are poorly correlated, having correlation coefficients lower than 0.4. This suggests that the spread of values is mostly due to random, rather than systematic, variation, although the fact that the correlation coefficients are all slightly positive suggests perhaps some small underlying systematic variation. The exceptions are correlations between B_{trace} and $E_{y,\text{sw}}$ and between $E_{x,\text{sc}}$ and $E_{x,\text{sw}}$, which have correlation coefficients larger than 0.8. This is due to the reasons discussed above: the $E_{y,\text{sw}}$ spectrum is essentially a measure of the B_{trace} spectrum because the y -component of the last term in Equation (2) is large and $E_{x,\text{sc}}$ and $E_{x,\text{sw}}$ are similar because the x -component of the last term in Equation (2) is not large (since \mathbf{v}_{sw} is mostly in the x -direction).

We have performed the first survey of electric field data in the solar wind to measure the perpendicular spectrum of inertial range fluctuations. It was found that there is a spread of spectral index values but that the average spectral index depends on the frame of measurement. In the spacecraft frame, the y -component of the electric field is primarily due to the magnetic field fluctuations being convected past the spacecraft at the average solar wind speed. It, therefore, has the same average spectral index (to within errors) as the magnetic field of -1.66 ± 0.01 . This is consistent with previous single interval electric field measurements in the spacecraft frame (Bale et al. 2005; Sahraoui et al. 2009). In the mean solar wind frame, the electric field is primarily due to velocity fluctuations in a mean magnetic field and has a spectral index of -1.40 ± 0.01 , which is closer to the velocity spectral index than the magnetic field spectral index, although not the same to within errors. The compressive fluctuations ($|\mathbf{B}|$ and n) were found to have the same spectral index as the magnetic field and not the velocity.

The difference between the scaling of the electric field in the spacecraft frame and the mean solar wind frame provides independent confirmation of the difference in scaling between the velocity and magnetic field. This difference is not expected for Alfvénic fluctuations, since $\delta\mathbf{v}$ is proportional to $\delta\mathbf{B}$ in an Alfvén wave, and is not predicted by any of the current theories of Alfvénic turbulence (although see recent work by Boldyrev et al. (2011) and Wang et al. (2011)). Recently, Roberts (2010) found that further out into the heliosphere, past 5 AU, the velocity spectral index evolves toward $-5/3$ to match the magnetic field. Although an important result, this does not explain the difference at 1 AU. Possible reasons for the difference include the effects of scale-dependent alignment, imbalance and residual energy and these will be investigated in a future paper.

This work was supported by NASA grant NNX09AE41G. We acknowledge the *THEMIS* team and NASA contract NAS5-02099. We thank J. Bonnell, J. McFadden, A. Schekochihin, and D. Sundkvist for useful conversations and an anonymous referee for helpful comments.

REFERENCES

- Angelopoulos, V. 2008, *Space Sci. Rev.*, 141, 5
 Angelopoulos, V. 2010, *Space Sci. Rev.*, doi:10.1007/s11214-010-9687-2
 Auster, H. U., Glassmeier, K. H., Magnes, W., et al. 2008, *Space Sci. Rev.*, 141, 235
 Bale, S. D., Kellogg, P. J., Mozer, F. S., Horbury, T. S., & Reme, H. 2005, *Phys. Rev. Lett.*, 94, 215002
 Belcher, J. W., & Davis, L. 1971, *J. Geophys. Res.*, 76, 3534
 Bellamy, B. R., Cairns, I. H., & Smith, C. W. 2005, *J. Geophys. Res.*, 110, 10104
 Beresnyak, A., & Lazarian, A. 2008, *ApJ*, 682, 1070
 Boldyrev, S. 2006, *Phys. Rev. Lett.*, 96, 115002
 Boldyrev, S., Perez, J. C., Borovsky, J. E., & Podesta, J. J. 2011, arXiv:1106.0700v1
 Bonnell, J. W., Mozer, F. S., Delory, G. T., et al. 2008, *Space Sci. Rev.*, 141, 303
 Bruno, R., & Carbone, V. 2005, *Living Rev. Sol. Phys.*, 2, 4
 Chandran, B. D. G. 2008, *ApJ*, 685, 646
 Chapman, S. C., & Hnat, B. 2007, *Geophys. Res. Lett.*, 34, L17103
 Chen, C. H. K., Horbury, T. S., Schekochihin, A. A., Wicks, R. T., Alexandrova, O., & Mitchell, J. 2010a, *Phys. Rev. Lett.*, 104, 255002
 Chen, C. H. K., Mallet, A., Yousef, T. A., Schekochihin, A. A., & Horbury, T. S. 2011, *MNRAS*, doi:10.1111/j.1365-2966.2011.18933.x
 Chen, C. H. K., Wicks, R. T., Horbury, T. S., & Schekochihin, A. A. 2010b, *ApJ*, 711, L79
 Goldreich, P., & Sridhar, S. 1995, *ApJ*, 438, 763
 Goldstein, M. L., Roberts, D. A., & Matthaeus, W. H. 1995, *ARA&A*, 33, 283
 Horbury, T. S., Forman, M., & Oughton, S. 2008, *Phys. Rev. Lett.*, 101, 175005
 Horbury, T. S., Forman, M. A., & Oughton, S. 2005, *Plasma Phys. Control. Fusion*, 47, B703
 Howes, G. G., Bale, S. D., Klein, K. G., et al. 2011, arXiv:1106.4327v1
 Issautier, K., Mangeney, A., & Alexandrova, O. 2010, in *AIP Conf. Proc.* 1216, Twelfth International Solar Wind Conference, ed. M. Maksimovic et al. (Melville, NY: AIP), 148
 Lithwick, Y., Goldreich, P., & Sridhar, S. 2007, *ApJ*, 655, 269
 Mangeney, A., Salem, C., Veltri, P. L., & Cecconi, B. 2001, in *Proc. ESA SP-492, Sheffield Space Plasma Meeting: Multipoint Measurements versus Theory*, ed. B. Warmbein (Noordwijk: ESA), 53
 Marsch, E., & Tu, C.-Y. 1990, *J. Geophys. Res.*, 95, 11945
 McFadden, J. P., Carlson, C. W., Larson, D., et al. 2008, *Space Sci. Rev.*, 141, 277
 Percival, D. B., & Walden, A. T. 1993, *Spectral Analysis for Physical Applications* (Cambridge: Cambridge Univ. Press)
 Perez, J. C., & Boldyrev, S. 2009, *Phys. Rev. Lett.*, 102, 025003
 Petrosyan, A., Balogh, A., Goldstein, M. L., et al. 2010, *Space Sci. Rev.*, 156, 135
 Podesta, J. J. 2011, *Phys. Plasmas*, 18, 012907
 Podesta, J. J., & Bhattacharjee, A. 2010, *ApJ*, 718, 1151
 Podesta, J. J., & Borovsky, J. E. 2010, *Phys. Plasmas*, 17, 112905
 Podesta, J. J., Roberts, D. A., & Goldstein, M. L. 2007, *ApJ*, 664, 543
 Roberts, D. A. 2010, *J. Geophys. Res.*, 115, 12101
 Sahraoui, F., Goldstein, M. L., Robert, P., & Khotyaintsev, Y. V. 2009, *Phys. Rev. Lett.*, 102, 231102
 Salem, C., Mangeney, A., Bale, S. D., & Veltri, P. 2009, *ApJ*, 702, 537
 Schekochihin, A. A., Cowley, S. C., Dorland, W., et al. 2009, *ApJS*, 182, 310
 Smith, C. W., Hamilton, K., Vasquez, B. J., & Leamon, R. J. 2006, *ApJ*, 645, L85
 Taylor, G. I. 1938, *Proc. R. Soc. A*, 164, 476
 Tessein, J. A., Smith, C. W., MacBride, B. T., et al. 2009, *ApJ*, 692, 684
 Tu, C.-Y., & Marsch, E. 1995, *Space Sci. Rev.*, 73, 1
 Wang, Y., Boldyrev, S., & Perez, J. C. 2011, arXiv:1106.2238v1
 Wicks, R. T., Horbury, T. S., Chen, C. H. K., & Schekochihin, A. A. 2010, *MNRAS*, 407, L31
 Wicks, R. T., Horbury, T. S., Chen, C. H. K., & Schekochihin, A. A. 2011, *Phys. Rev. Lett.*, 106, 045001